International Journal of Food Science +Technology

Institute of Food Science +Technology ifst

Original article

Optimising chitosan–pectin hydrogel beads containing combined garlic and holy basil essential oils and their application as antimicrobial inhibitor

Kittikoon Torpol,[1] Sujinda Sriwattana,[1]* Jurmkwan Sangsuwan,[2] Pairote Wiriyacharee[1] & Witoon Prinyawiwatkul[3]

1 Division of Product Development Technology, Faculty of Agro-Industry, Chiang Mai University, Chiang Mai 50100, Thailand
2 Division of Packaging Technology, Chiang Mai University, Chiang Mai 50100, Thailand
3 School of Nutrition and Food Sciences, Louisiana State University Agricultural Center, Baton Rouge, LA 70803, USA

(Received 12 November 2018; Accepted in revised form 7 January 2019)

Summary Chitosan–pectin hydrogel beads that trap and release the maximal amount of combined garlic and holy basil essential oils to inhibit food microorganisms were developed based on the central composite design, with chitosan (0.2–0.7% w/v), pectin (3.5–5.5% w/v) and calcium chloride ($CaCl_2$) (5.0–20.0% w/v) contents. The optimal bead consisted of 0.3–0.6% w/v chitosan, 3.9–5.1% w/v pectin and 8.0–17.0% w/v $CaCl_2$, which had a high encapsulation efficiency (62.16–79.06%) and high cumulative release efficiency (31.55–37.81%) after storage at 5 °C for 15 days. Optimal hydrogel beads were packed into a cellulose bag to evaluate antimicrobial activity by the disc volatilisation method. The beads inhibited *Bacillus cereus*, *Clostridium perfringens*, *Escherichia coli*, *Pseudomonas fluorescens*, *Listeria monocytogenes* and *Staphylococcus aureus* but did not affect *Lactobacillus plantarum* and *Salmonella* Typhimurium. The oil-containing beads could potentially be applied in food packaging to inhibit the mentioned microorganisms.

Keywords Antimicrobial beads, chitosan-pectin hydrogel beads, essential oils, garlic, holy basil, optimisation.

Introduction

It is well recognised that some essential oils (EOs) effectively inhibit a wide range of food microorganisms (Calo *et al*., 2015) *in vitro* and in complex food systems (Shah *et al*., 2013). The EOs from garlic (*Allium sativum*, family Liliaceae), GEO, and holy basil (*Ocimum sanctum*, family Lamiaceae), HBEO, are commonly used in food products (Raut & Karuppayil, 2014). While the single EOs display a certain degree of antimicrobial activity, the synergistic actions of mixed oil fractions are often exploited to improve the potency and antimicrobial activity spectrum of the individual oils (Nedorostova *et al*., 2009; Boukhatem *et al*., 2013). For instance, GEO alone inhibited *Bacillus cereus*, *Clostridium perfringens*, *Pseudomonas fluorescens*, *Salmonella* Typhimurium and *Staphylococcus aureus* but had no effect on *Escherichia coli*, *Listeria monocytogenes*, *Lactobacillus plantarum*, however, the 1:1 ratio of GEO (containing diallyl di- and trisulphides [DADS and DATS, respectively]) and HBEO (containing eugenol, methyl eugenol and caryophyllene) inhibited all the bacteria tested (Torpol *et al*., 2018).

Comprising a diverse collection of lipophilic and highly volatile constituents, EOs are well recognised as being susceptible to chemical deterioration upon exposure to extrinsic parameters, notably, light, temperature and oxygen availability (Bustamante *et al*., 2017). Moreover, the direct application of EOs into food is limited because their pungent flavour and odour can affect the food perception (Nielsen *et al*., 2017). To overcome these technical challenges, microencapsulation, the process by which small discrete solid particles or small liquid droplets are surrounded and enclosed within a protective outer layer (Benavides *et al*., 2016), is notable for providing immobilisation, stability and controlled release of sensitive compounds (Bannikova *et al*., 2017). The particles comprise a core material as the internal phase, and a wall material as the coating phase (Bakry *et al*., 2016). Ionic gelation forms hydrogel by interaction between a charged polymer and an ion divalent with oppositely charge (Kim *et al*., 2017; de Moura *et al*., 2018). This technique can not only

*Correspondent: Fax: +66 53 948 230;
e-mails: sujinda.s@cmu.ac.th or sujindapdt@gmail.com

doi:10.1111/ijfs.14107

defend against volatilisation losses of EOs (Benavides *et al*., 2016) but also provide a porous matrix for releasing the active compounds (Singh *et al*., 2017).

Hydrogels are three-dimensional cross-linked polymer networks, which can absorb large amounts of water (Ahmed, 2015). These networks maintain their structure during the exchange of water and provide controlled release via pores in the polymer network (Zhu *et al*., 2018). Hydrogels based on polysaccharides, like chitosan and pectin, have been increasingly utilised in various fields (Kwiecień & Kwiecień, 2018). Since chitosan is positively-charged in low pH conditions (pH below its pK_a), it spontaneously associates with negatively-charged polyanions in solution to form polyelectrolyte complexes (Kim *et al*., 2017), which are favourable excipients in controlled release delivery systems (He *et al*., 2016). Pectin is an anionic heteropolysaccharide that mainly consists of linearly linked $\alpha(1\rightarrow4)$-D-galacturonic residues, with varying amounts of methyl-esterified carboxyl groups (Konovalova *et al*., 2017).

Sachets containing microencapsulated beads with an EO core are new alternatives with antimicrobial properties and can be applied in food packaging systems to release the active compounds onto the food surface (Chang *et al*., 2017). This approach avoids directly fortifying food with the EO (Lu *et al*., 2016), thereby maintaining the food integrity and its sensory qualities (Haghighi-Manesh & Azizi, 2017). In this research, chitosan–pectin hydrogel beads were developed for the entrapment of GEO and HBEO with high encapsulation and release efficiency, and their antimicrobial effect against selected microorganisms was evaluated.

Materials and methods

Materials

Chitosan from shrimp (size <40 mesh, low molecular weight with 94.87% deacetylation) was purchased from Ta Ming Enterprises Co. Ltd., Samut Sakhon, Thailand. Pectin from citrus peel (commercial grade low-methoxy pectin with 2.9% degree of esterification) was purchased from CP Kelco, Lille Skensved, Denmark. Calcium chloride ($CaCl_2$) was purchased from Merck, Damstadt, Germany. GEO and HBEO were purchased from Chemipan Co. Ltd., Bangkok, Thailand. All other chemicals and reagents were of analytical grade.

Volatile composition

GEO+HBEO was prepared at 1:1 v/v ratio in a brown glass bottle to provide light protection and analysed for its volatile compounds, using gas chromatography–mass spectrometry–solid-phase microextraction (GC–MS–SPME) (Calvo-Gómez *et al*., 2004; Sriwattana *et al*., 2015; Yamani *et al*., 2016). Combined GEO+HBEO (0.5 mL) or 2.20 g beads were added into vials, and an SPME fibre coated with 100 μm of polydimethylsiloxane was inserted into the headspace of the sample vials. After extraction at 25 °C for 30 min, SPME fibre with adsorbed volatile components was inserted into the injection port of a GC–MS instrument (model GC-7890A, Hewlett-Packard, Santa Clara, CA, USA) equipped with a DB-5 capillary column (30 m, 0.25 mm I.D., 0.25 μm film thickness) and MS detector (MSD 5975C), and the volatiles identified and quantified according to the method of Torpol *et al*. (2018).

Preparation of chitosan–pectin hydrogel beads containing essential oils (EOs)

Chitosan–pectin hydrogel beads were prepared using ionic gelation via the dripping method (Sangsuwan *et al*., 2016) with some modifications. $CaCl_2$ was dissolved in deionised water at room temperature. The pectin was dissolved in deionised water at 40 °C using a magnetic stirrer. Chitosan was dissolved in 5% (v/v) acetic acid at 70 °C. Once completely dissolved, pectin and chitosan were cooled to 35 °C. Combined GEO+HBEO (1:1 v/v) were added to the pectin solution and the mixture homogenised for 5 min in the presence of 0.5% (v/v) Tween 20, as an emulsifying agent. The pectin-containing oil was loaded into a syringe and dripped into $CaCl_2$ at 35 ± 1 °C under magnetic stirring for 30 min. After washing with deionised water, the beads were immersed in chitosan for 30 min. The beads were re-washed, oven-dried at 60 °C (Nazarudin *et al*., 2011; Bahmani *et al*., 2015) for 4 h, packed in an aluminium foil bag, and kept at 4–6 °C for further analysis.

Experimental design

According to our preliminary study, the chitosan content should not exceed 0.70% (w/v) since above this level, it caused high viscosity, resulting in beads floating on the surface. In addition, a pectin content over 5.50% (w/v) led to a highly viscous solution, making it difficult to dispense from the syringe. The combined GEO+HBEO (1:1) at 1.50% (v/v) (Torpol *et al*., 2018) was used in this study. A central composite design (CCD) for three numeric factors: chitosan, 0.20–0.70% (w/v); pectin, 3.50–5.50% (w/v); $CaCl_2$, 5.00–20.00% (w/v) (Bera *et al*., 2009; Khan & Bajpai, 2011), with one replication of the factorial point and axial point, respectively, and three centre points with alpha at -1.682, +1.682, and, hence, a total of 17 runs (Hu, 1999), was used in this study. The experiment data were fitted to a second-order polynomial equation,

which described the relationship between the antimicrobial activity (independent variable) and the three test variables (dependent variables).

$$Y_i = \beta_0 + \beta_1 X_1 + \beta_2 X_2 + \beta_3 X_3 + \beta_{11} X_1^2 + \beta_{22} X_2^2 + \beta_{33} X_3^2 + \beta_{12} X_1 X_2 + \beta_{13} X_1 X_3 + \beta_{23} X_2 X_3 \quad (1)$$

where Y_i is the dependent variable; β_0, a constant; β_1, β_2 and β_3, linear coefficients; β_{11}, β_{22} and β_{33}, quadratic coefficients; β_{12}, β_{13} and β_{23}, interaction coefficients, and X_1, X_2 and X_3, the independent variables (chitosan, pectin and $CaCl_2$, respectively). The model performance was evaluated by the coefficient of determination (R^2), the significance of the model analysis ($P \leq 0.05$) and the lack-of-fit test (Bagheri *et al.*, 2014). The encapsulation efficiency (%EE) and cumulative release efficiency (%CRE) were used to derive the optimal bead composition.

Determination of the oil amount in chitosan–pectin hydrogel beads

The amount of EO in the hydrogel beads was determined by spectrophotometric measurements (UV-1800, Shimadzu, Japan) at the maximum absorption wavelength ($\lambda = 281$ nm), using the standard calibration curve method (Peng *et al.*, 2014; Sangsuwan *et al.*, 2016). A standard curve was constructed by serial dilution of the combined oils (GEO+HBEO at 1:1 v/v) with 80% (v/v) ethanol to obtain concentrations over the range of 0.00001–0.00015 mL per 100 mL ethanol. The linear regression equation ($y = 7984x–0.02927$, $R^2 = 0.994$) was used to calculate the oil concentration for %EE and %CRE.

Encapsulation efficiency (%EE) and cumulative release efficiency (%CRE)

A precise weight of dried beads was dripped into 50 mL of 80% (v/v) ethanol for 1 h at room temperature, sonicated (Elma, Germany) at 60 °C for 30 min and left overnight at room temperature. After filtering, the absorbance of the solution was measured at 281 nm. The absorbance values were used to calculate the %EE, using the linear regression equation. The % EE was calculated according to the following equation (Yang *et al.*, 2014):

$$\mathrm{EE}(\%) = \frac{v_1}{v_2} \times 100\% \quad (2)$$

where EE is encapsulation efficiency (%); and v_1 and v_2 are the total volume of oil used in bead preparation and the volume of oil after extraction, respectively.

A precise weight of dried hydrogel beads was incubated at 5 °C and 87.67% relative humidity, provided by saturated potassium chloride solution, for 15 days. The oil remaining in the beads on day 15 was extracted, and the amount determined according to the linear regression equation. The %CRE was calculated as follows (Peng *et al.*, 2014):

$$\mathrm{CRE}(\%) = \frac{r1 - r2}{r1} \times 100\% \quad (3)$$

where r_1 and r_2 are the oil contents in the beads before and after storage, respectively.

Beads morphology

The surface, cross-section and internal core of the optimal chitosan–pectin beads containing combined GEO+HBEO were examined by scanning electron microscopy (JEOL-JSM6360, Japan) at 15 kV. Before the analysis, the samples were dried with CO_2 and gold-coated.

Assessment of the functional groups by FTIR

Dried samples of chitosan, pectin, optimal chitosan–pectin beads without EO, and optimal chitosan–pectin beads containing combined GEO+HBEO were prepared with potassium bromide. Fourier transform infrared (FTIR) spectra were recorded (Perkin Elmer2000, Waltham, MA, USA) in the range of 400 to 4000 cm^{-1}.

Antimicrobial activity of chitosan-pectin hydrogel beads containing combined garlic and holy basil oils against selected bacteria

The cellulose paper was cut to obtain a small bag (3.0 × 4.0 cm), which was heat-sealed on three sides using an impulse bag sealer and placed in a hot air oven at 105 °C, for 1 h. Beads at different weights (0.55, 1.10, 2.20 and 4.40 g) were packed in the cellulose bags and immediately sealed. The antimicrobial activity of chitosan–pectin hydrogel beads containing combined oils was performed using a modified disc volatilisation method (Boukhatem *et al.*, 2013; Torpol *et al.*, 2018). Eight bacterial strains, including five Gram-positive bacteria (*B. cereus*, *C perfringens* ATCC 13124, *Lb. plantarum* TISR863, *L. monocytogenes* DMST 17303, *S. aureus* ATCC 25923) and three Gram-negative bacteria (*E. coli* ATCC 25922, *P. fluorescens*, *S.* Typhimurium ATCC 13311), all obtained from the Clinical Microbiology Department, Faculty of Associated Medical Science, Chiang Mai University, Thailand, were used. The tested concentration of bacterial suspension was 0.5 McFarland (10^8 CFU/mL). Five mL of bacteria suspension was transferred to a Petri dish containing the specific media; the bag comprising the beads was attached under the upper lids of

the Petri dish and sealed with parafilm. *Bacillus cereus*, *E. coli*, *P. fluorescens*, *S.* Typhimurium and *S. aureus* strains were inoculated onto Mueller–Hinton agar (MHA), *C. perfringens* and *L. monocytogenes* onto Mueller–Hinton blood agar (MHBA), and *Lb. plantarum* onto de Man–Rogosa–Sharpe (MRS). *Clostridium perfringens* was inoculated and kept under anaerobic conditions while *L. monocytogenes* and *Lb. plantarum* were held in a CO_2 incubator. After incubation at 37 °C for 48 h, the diameter (mm) of the clear zone was measured with a calliper.

Statistical analysis

Response surface methodology was applied to the experiment data, using the Design Expert statistical package trial version 10 (Stat-Ease, Inc., Minneapolis, MN, USA). The criteria to obtain the optimal region were maximum %EE and %CRE. One optimal point was then selected, based on the lowest cost of the formulation. An analysis of variance (ANOVA) was applied to test differences in clear zones among treatments. Differences between treatments were identified by Duncan's new multiple range test ($\alpha = 0.05$). All data were analysed using SPSS 16.0 software (SPSS, Inc., Chicago, IL, USA).

Results and discussion

Volatile compositions of essential oil (EO)

The volatile components of the combined oils (GEO+HBEO at 1:1 v/v) and their relative contributions (peak area percentages) were determined by GC–MS. The major compositions of the oils are shown in Table 1. The vapour of GEO+HBEO before encapsulation consisted of eugenol (12.30%), caryophyllene (10.27%), diallyl tetrasulphide (DATTS) (4.80%) and α-caryophyllene (2.04%) while the main components of GEO+HBEO released from beads were eugenol (6.24%), caryophyllene (6.20%), α-caryophyllene (1.20%) and DATTS (0.26%). As can be seen, the peak area percentages of the major compounds extracted from beads were lower than those of the pure combined oils. Loss of the volatile compounds may be affected by other factors besides the conditions used to prepare hydrogel beads, which should be further investigated in the future experiment.

Table 1 The major compositions of combined garlic+holy basil essential oils (at a 1:1 v/v ratio) identified[a] and quantified using gas chromatography–mass spectrometry

Component	Percentage in samples (%)	
	Vapour sample[b]	Hydrogel bead sample[b]
Eugenol	12.30	6.24
Caryophyllene	10.27	6.20
α-Caryophyllene	2.04	1.20
Diallyl tetrasulphide (DATTS)	4.80	0.26

[a]Expressed as %peak area. Other negligible identified compounds are not listed.

[b]Extracted by solid-phase microextraction.

A previous study (Torpol *et al.*, 2018) showed that HBEO contained eugenol (49.87%) and caryophyllene (4.96%) as main components, however, DADS (31.67%), DATS (31.56%) and DATTS (13.48%) were the major fractions in GEO. Consequently, the combined GEO+HBEO (1:1 v/v) was potentially a strong antimicrobial inhibitor because HBEO contributed a large percentage of eugenol and caryophyllene as inhibitory agents, and DATTS was a key fraction of GEO. Phanthong *et al.* (2013) reported that eugenol, caryophyllene and methyl eugenol in HBEO were key compounds to inhibit *B. cereus*, *E. coli*, *S. aureus* and *S.* Typhimurium. Furthermore, many studies suggested that DATTS provided a potent antimicrobial activity (Rattanachaikunsopon & Phumkhachorn, 2008). The antimicrobial potential of GEO has been demonstrated to increase with the number of disulphide groups, corresponding to relative MIC values of DATTS < DATS < DADS, in controlling *B. cereus*, *L. monocytogenes*, *S. aureus* and *E. coli* (Naganawa *et al.*, 1996; Rattanachaikunsopon & Phumkhachorn, 2008). Therefore, chitosan–pectin hydrogel beads loaded with GEO+HBEO at 1:1, v/v could expectedly inhibit a wide range of microorganisms.

Development of chitosan–pectin hydrogel beads containing essential oils (EOs)

The 17 treatments were accomplished by ionic gelation via the dripping method. All formulations showed %EE values in the range of 35.44–76.64%, and %CRE in the range of 12.69–45.63%, respectively (Table 2). The second-order polynomial model was significant ($P \leq 0.05$) and the lack-of-fit was insignificant ($P > 0.05$), confirming the estimated model fit well the experiment data (Getachew & Chun, 2016). The effects of three factors levels on the responses were evaluated using the full models presented in eqns (4) and (5).

$$\%EE = 51.28 + 4.76X_1 + 10.11X_2 - 1.00X_3 - 7.73X_1X_2 + 4.22X_2X_3 - 2.88X_1X_3 + 4.89X_1^2 + 2.27X_2^2 - 0.56X_3^2 \quad (4)$$

Table 2 Response surface central composite design and results for variables

Run	Independent variables			Dependent variables[a]	
	*X*1 (chitosan) (% w/v)	*X*2 (pectin) (% w/v)	*X*3 ($CaCl_2$) (% w/v)	*Y*1 (%EE)	*Y*2 (%CRE)
1	(−1) 0.30	(−1) 3.90	(−1) 8.00	37.72	15.12
2	(+1) 0.60	(−1) 3.90	(−1) 8.00	53.13	21.00
3	(−1) 0.30	(+1) 5.10	(−1) 8.00	74.43	33.16
4	(+1) 0.60	(+1) 5.10	(−1) 8.00	67.06	28.87
5	(−1) 0.30	(−1) 3.90	(+1) 17.00	36.20	19.00
6	(+1) 0.60	(−1) 3.90	(+1) 17.00	76.64	45.63
7	(−1) 0.30	(+1) 5.10	(+1) 17.00	69.54	15.00
8	(+1) 0.60	(+1) 5.10	(+1) 17.00	70.91	18.10
9	(−1.682) 0.20	(0) 4.50	(0) 12.50	56.59	25.81
10	(+1.682) 0.70	(0) 4.50	(0) 12.50	65.63	35.00
11	(0) 0.45	(†1.682) 3.50	(0) 12.50	35.92	12.69
12	(0) 0.45	(+1.682) 5.50	(0) 12.50	71.52	36.79
13	(0) 0.45	(0) 4.50	(−1.682) 5.00	56.00	15.73
14	(0) 0.45	(0) 4.50	(+1.682) 20.00	35.44	19.41
15	(0) 0.45	(0) 4.50	(0) 12.50	49.29	32.22
16	(0) 0.45	(0) 4.50	(0) 12.50	53.88	34.46
17	(0) 0.45	(0) 4.50	(0) 12.50	52.04	30.10

[a]Encapsulation efficiency (%EE) and Cumulative release efficiency (%CRE).

$$\%\mathrm{CRE} = 32.21 + 3.42X_1 + 2.56X_2 + 0.42X_3 - 4.21X_1X_2 + 3.52X_2X_3 - 7.18X_1X_3 - 0.49X_1^2 - 2.50X_2^2 - 5.03X_3^2. \quad (5)$$

Based on ANOVA, the full models showed slightly higher adjusted R^2 values compared to the reduced models for %EE (0.68 vs. 0.67) and %CRE (0.62 vs. 0.58). Therefore, they were used to optimise the formulation.

Table 3 and Figure S1 show that the %EE value was significantly influenced by the linear terms of pectin and the interaction of chitosan with pectin ($P \leq 0.05$). Pectin positively affected the %EE because this biopolymer was used as the core material in the hydrogel beads structure developed by the ionic gelation method. Kim *et al.* (2003) noted that the loading efficiency of albumin in chitosan-coated pectin beads was affected by the weight ratio of pectin-to-albumin and the concentration of $CaCl_2$. The extent of the cross-linking during gelation relies on the interaction between the negatively-charged pectin (COO^-) and positively-charged calcium ions (Ca^{2+}) (Pawar *et al.*, 2008; Jaya *et al.*, 2009). These intermolecular associations induce the formation of a three-dimensional structure at low pHs (Bannikova *et al.*, 2017). Accordingly, El-Kamel *et al.* (2003) noted that the drug loading efficiency of calcium alginate beads was directly proportional to the polymer concentration, owing to the enhanced availability of active calcium-binding sites and, thereby the more extensive cross-linking as the quantity of alginate increased. Conversely, increasing the calcium ion concentration can lead to possible saturation of the calcium-binding sites in the polymer chain, preventing further calcium ion entrapment, and so the cross-linking might not be altered by increasing the concentration of the calcium chloride solution (El-Kamel *et al.*, 2003). However, in this study, increasing the calcium concentration did not affect the %EE. In addition, the %CRE was mainly affected by the interaction between pectin and $CaCl_2$, and the quadratic coefficient of $CaCl_2$ ($P \leq 0.05$). Analysis of drug dissolution from calcium pectinate beads has previously revealed that internal cross-linked beads compacted the core, which decreased the drug release by 10–20% when compared to counterparts undergone cross-linking of the surface (Pawar *et al.*, 2008). Chitosan-coated beads were also expected to delay the release rate (Shi *et al.*, 2008; Kim *et al.*, 2003).

By analysis of the response surface plots (Figure S1), the optimal bead formulation to maximise the %EE and %CRE responses comprised 0.3–0.6% w/v chitosan, 3.9–5.1% w/v pectin and 8.0–17.0% w/v $CaCl_2$. It showed that a high pectin content provided a high %EE. Chitosan and $CaCl_2$ levels were selected, based on the price of the formulation. Therefore, the selected composition was 0.3% chitosan, 5.1% pectin and 8.0% $CaCl_2$, which yielded the predicted 79.06%EE and 37.81%CRE (Table 4). An optimal formulation was produced, validated and analysed for all

Table 3 Regression coefficients of chitosan–pectin hydrogel beads predicted model

	%EE[a]		%CRE[b]	
Independent variable	**Estimated coefficient**	**$P \leq 0.05$**	**Estimated coefficient**	**$P \leq 0.05$**
Model	51.28	0.0343*	32.21	0.0450*
X_1 (chitosan)	4.76	0.0758	3.42	0.0710
X_2 (pectin)	10.11	0.0031*	2.56	0.1562
X_3 ($CaCl_2$)	−1.00	0.6757	0.42	0.8005
X_1X_2 (chitosan×pectin)	−7.73	0.0361*	−4.21	0.0853
X_1X_3 (chitosan×$CaCl_2$)	4.22	0.2009	3.52	0.1383
X_2X_3 (pectin×$CaCl_2$)	−2.88	0.3676	−7.18	0.0112*
X_1^2(chitosan^2)	4.89	0.0934	−0.49	0.7890
X_2^2 (pectin^2)	2.27	0.3962	−2.50	0.2019
X_3^3 ($CaCl_2{}^2$)	−0.56	0.8318	−5.03	0.0251*

[a]Encapsulation efficiency (%EE).
[b]Cumulative release efficiency (%CRE).
*Significant level at 95% ($P \leq 0.05$).

responses. Table 4 verifies that the experiment values of %EE and %CRE did not significantly differ ($P \leq 0.05$) from the predicted values. Since the absolute percentage of approximated error of %EE and % CRE were below 10%, being in the range of 2.13–5.71%, there was good agreement between the predicted and measured values (Hu, 1999).

Beads morphology

The dried optimal beads were globular with a diameter of 1.65–2.86 mm. The morphology of the optimal chitosan–pectin bead, observed by SEM (Fig. 1), showed the smooth bead surface, and the internal structure had small holes and some cracks, due to the drying process. Previous work noted that chitosan-coated alginate/poly(*N*-isopropylacrylamide) beads provided a smooth surface relative to the uncoated beads (Shi *et al*., 2008). Furthermore, vacuoles in the matrix may increase the amount of EO trapped within the beads (Sutaphanit & Chitprasert, 2014).

Table 4 Comparison of response values of predicted and experimental data of optimal hydrogel beads

	Response values		
Beads properties	**Predicted**	**Experimental**	**% error**
Encapsulation efficiency (%)	79.06	$77.38^{ns} \pm 1.76$	2.13
Cumulative release efficiency (%)	37.81	$35.65^{ns} \pm 0.90$	5.71

Response values of experimental are given as mean ± standard deviation of three replications.
ns = not significant level in same row ($P \leq 0.05$) using the Student's *t*-test.

Assessment of the functional groups by FTIR

FTIR was used to identify the presence of chitosan and pectin based on their functional groups (Fig. 2) and to compare the blank (non-loaded) optimal bead with those containing combined GEO+HBEO. The FTIR spectra of pectin showed a peak at 1736.4 cm^{-1}, representing carbonyl (C=O) bonds (Fig. 2b). For pectin–chitosan hydrogel beads, the peak shifted to a new broad band at 1725.4 cm^{-1} (Fig. 2c) due to the interaction of the negatively-charged COO^- groups of pectin with the positively-charged Ca^{2+} ions. The peak characteristic of pectin–mefenamic acid film with $CaCl_2$ was observed by C=O stretching at 1723 cm^{-1} (Moreira *et al*., 2014). The FTIR spectra of chitosan showed typical bands for C=O vibrations of the acetylated units (-$CONH_2$ groups), and protonated amino groups at 1584.2 cm^{-1} (amide II, Fig. 2a). After chitosan was coated on pectin beads, the chitosan band (amide II) shifted to 1513.9 cm^{-1} (Fig. 2c) as a result of pectin–chitosan interactions. Previous studies suggested that the amide II band of chitosan shifted to lower wavelengths because of alginate–chitosan interactions (Deladino *et al*., 2008; Vasile *et al*., 2016). de Souza *et al*. (2009) noticed some changes in the spectra of pectin beads at 1560–1561 cm^{-1} after reacetylation of chitosan transforms to amide groups.

Allium sativum contains a variety of compounds, with a particular emphasis on flavonoids, saponins, sapogenins and organosulfur compounds (Molina-Calle *et al*., 2017). In the FTIR spectra, the peaks at 3265–3339 and 3462 cm^{-1} (strong for GEO) signifies the O-H stretching vibrations of hydroxyl groups, which is attributed to polyhydroxy compounds, such as flavonoids, non-flavonoids and saponins (Katata-Seru *et al*., 2017). Asymmetric stretching of C-H groups of aromatic compounds (2926–2979 cm^{-1}) and the O-H bending of carboxylic acids

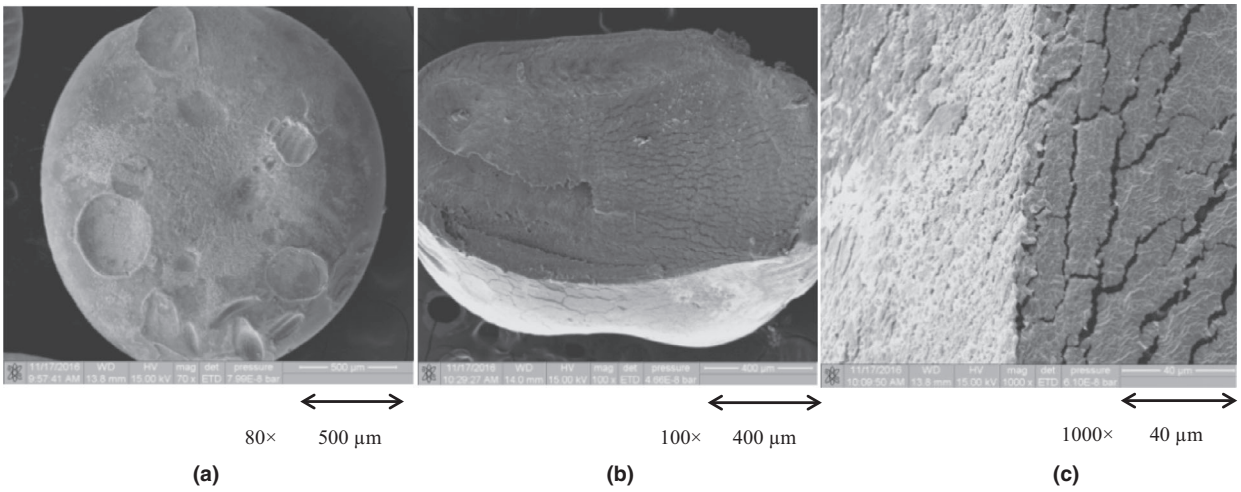

Figure 1 Scanning electron micrographs of the optimal chitosan-coated pectin hydrogel beads; (a) whole bead, (b) cross-section (c) surface.

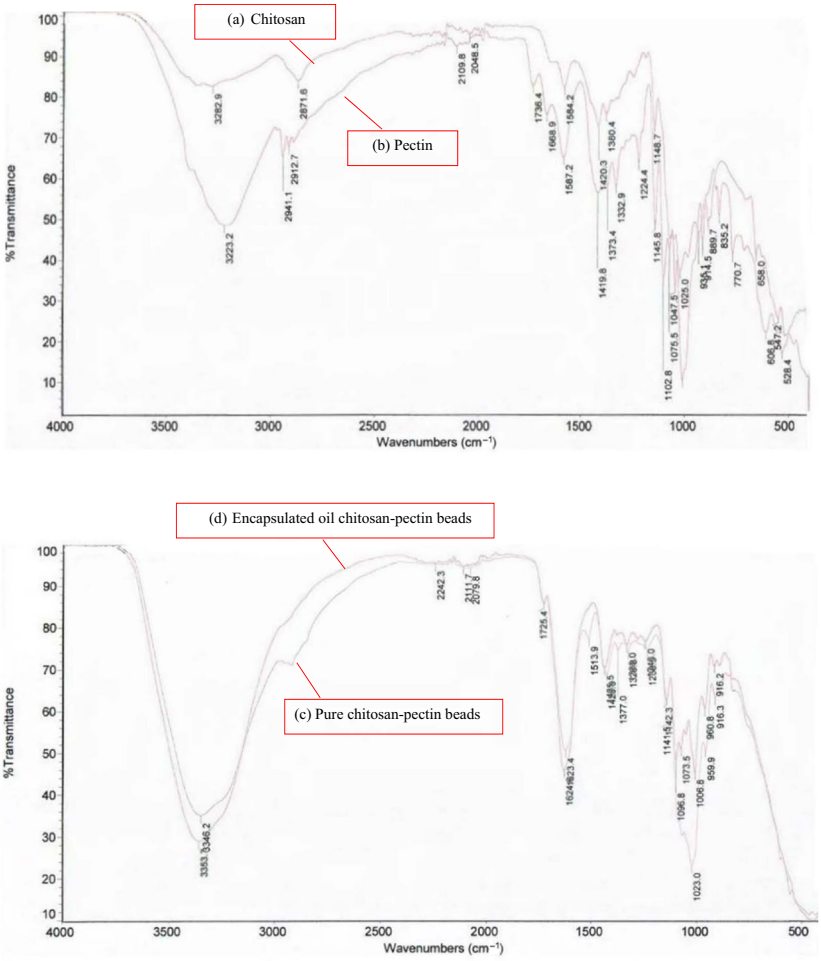

Figure 2 FTIR spectrum of chitosan (a), pectin (b), pure chitosan–pectin beads (c) and encapsulated oil chitosan–pectin beads (d).

(1384–1395 cm^{-1}) (Trifunschi *et al.*, 2015; Divya *et al.*, 2017) was seen, as well as the S=O group (1036 cm^{-1}) corresponding to organosulphur compounds, including alliin, allicin and DADS (Divya *et al.*, 2017). Characteristic vibration frequencies in the FTIR of *O. sanctum* are attributed to O-H groups (3369–3428 cm^{-1}), C=C

stretching vibrations in the aromatic rings (1509–1612 cm^{-1}) (Balamurughan *et al*., 2014; Sutaphanit & Chitprasert, 2014), C-H bending vibrations (1450 cm^{-1}), and O-H bending vibrations in phenols (1268 cm^{-1}). As mentioned earlier, HBEO primarily consists of eugenol, methyl eugenol and caryophyllene (Khan *et al*., 2010; Pandey *et al*., 2014). HBEO showed its dominant peaks at 1510, 1610 and 1640 cm^{-1}, corresponding to C-C stretching of the alkene/aromatic groups in the oil structure (Sajomsang *et al*., 2012; Sutaphanit & Chitprasert, 2014).

The chemical groups in the structure of the optimal beads (Fig. 2c) were similar to those present in pectin (Fig. 2b), which was used as the main structural component. It was also possible to observe that the chemical groups of the optimal beads were not changed after coating with chitosan, probably because the chitosan coating accumulated only at the surface of the beads. Furthermore, after incorporation of combined GEO+HBEO in beads, most of the characteristic peaks remained unchanged, suggesting that it was stable during the gelation method and drying process (Fig. 2d). The peak at 1509 cm^{-1} (C=C stretching vibration in aromatic ring) was slightly shifted to 1623.4 cm^{-1}, and the peaks at 1036 (S=O bonds in organosulphur compounds) and 1395 cm^{-1} (O-H bonds in carboxylic groups) were slightly shifted to 1023 and 1377 cm^{-1}, respectively. These results imply the GEO+HBEO might not chemically interact with the polymer of the hydrogel beads.

Antimicrobial activity of chitosan–pectin hydrogel beads containing combined oils against selected bacteria

The disc volatilisation method was used to evaluate the antimicrobial activity of optimal beads containing combined GEO+HBEO against selected bacterial strains, by packing the beads in cellulose bags (Table 5). It was evident that the clear zone increased as the bead weight increased ($P \leq 0.05$). The beads at 0.55, 1.10, 2.20 and 4.40 g corresponded to loaded GEO+HBEO volumes of 0.22, 0.44, 0.88, 1.56 mL, respectively. Although 0.55 g beads did not inhibit any of the bacteria studied, 1.10 g beads started to inhibit *B. cereus*, *Cl. perfringens* and *L. monocytogenes* (clear zone diameter of 14.00–33.33 mm). Furthermore, 2.20 g beads increased the inhibition zones (clear zone diameter 20.67–45.00 mm) for Gram-positive bacteria, including *B. cereus*, *Cl. perfringens* and *S. aureus*, and Gram-negative bacteria, such as *E. coli*, *L. monocytogenes* and *P. fluorescens*, were inhibited but not *Lb. plantarum* and *S. Typhimurium*. However, beads at 4.40 g showed the best antimicrobial activity (clear zone diameter 34.33–49.67 mm), although *Lb. plantarum* and *S.* Typhimurium had no inhibition zone. A previous article showed that the antimicrobial capacity of an EO-containing film was increased by the oil concentration (Zhang *et al*., 2017). Moreover, the combination of GEO+HBEO at 1:1 (v/v) affected Gram-positive bacteria more than Gram-negative bacteria when evaluated by the volatilisation method (Torpol *et al*., 2018). Therefore, the effect of chitosan–pectin hydrogel beads containing GEO+HBEO were expected to exhibit a greater inhibition of Gram-positive bacteria than Gram-negative bacteria as observed in this study.

Eugenol, a major component in HBEO, is a short-chain phenylpropanoid compound that can permeate the bacterial cell membrane to interact with proteins and increase the transport of potassium and ATP out of the cell, while allicin in GEO is readily transported across the cell membrane into the cytoplasm (Chouhan

Table 5 Inhibition zone (mm) of different beads in the cellulose bags (containing 0.55, 1.10, 2.20 and 4.40 g of beads) by disc volatilisation method

	Inhibition zone (mm)*			
Bacterial tested	**0.55 g beads**	**1.10 g beads**	**2.20 g beads**	**4.40 g beads**
Gram-positive				
Bacillus cereus	0.00^{d}	$14.00^{c} \pm 1.00$	$20.67^{b} \pm 0.76$	$43.33^{a} \pm 0.76$
Clostridium perfringens	0.00^{d}	$33.33^{c} \pm 1.04$	$42.00^{b} \pm 1.00$	$44.33^{a} \pm 0.58$
Staphylococcus aureus	0.00^{c}	0.00^{c}	$45.00^{b} \pm 1.00$	$49.67^{a} \pm 0.29$
Lactobacillus plantarum	0.00	0.00	0.00	0.00
Gram-negative				
Escherichia coli	0.00^{c}	0.00^{c}	$30.67^{b} \pm 0.29$	$34.33^{a} \pm 0.58$
Listeria monocytogenes	0.00^{d}	$23.38^{c} \pm 0.77$	$41.33^{b} \pm 0.76$	$44.00^{a} \pm 1.00$
Pseudomonas fluorescens	0.00^{d}	0.00^{d}	$34.33^{b} \pm 0.76$	$41.67^{a} \pm 0.57$
Salmonella Typhimurium	0.00	0.00	0.00	0.00

Letters in the same row represent statistically different results at Duncan's new multiple range test ($P \leq 0.05$).
*Diameters of inhibition zone are given as mean ± standard deviation of three replications.

et al., 2017). The antimicrobial activity of allicin is ascribed to its reactive chemical group that binds to and inhibits a broad range of intracellular targets by the interaction of -S(O)-S- groups of allicin with sulphydryl (-SH) groups of enzymes (Hyldgaard *et al*., 2012). Hence, the combined GEO+HBEO in chitosan–pectin hydrogel beads could inhibit the growth of selected microorganisms in this study.

When microencapsulated oregano oil was placed in the sachet bag, it effectively inhibited *Dickeya chrysanthemi*, moulds and yeasts, and total mesophilic aerobic bacteria on the surface of iceberg lettuce (Chang *et al*., 2017). Furthermore, the sachet of oregano EO displayed an inhibitory action against *E. coli*, *S.* Enteritidis and *Penicillium* sp. on sliced bread (Passarinho *et al*., 2014). Moreover, *L. monocytogenes*, lactic acid bacteria and total aerobic bacteria on mozzarella cheese were reduced by an antimicrobial sachet containing rosemary oil and thyme oil compared to untreated samples; although the flavour altered the odour perception (Han *et al*., 2014). Another study demonstrated that when chitosan beads containing lavender oil and thyme oil were placed inside a strawberry packaging system, the beads released the volatile oil to control *Botrytis cinerea*, and extended the storage life of strawberry, with no impact on the appearance, colour and firmness, besides scoring higher in the sensory test than the control sample (Sangsuwan *et al*., 2016). Therefore, the GEO+HBEO-containing beads could potentially be applied in food packaging as a microorganism inhibitor.

Conclusion

Pectin beads containing combined GEO+HBEO were coated with chitosan and gelled by $CaCl_2$ using the ionic gelation method. SEM revealed the beads were uniform with a globular shape and smooth surface of chitosan coating. The GEO+HBEO encapsulated in chitosan–pectin hydrogel beads were protected and did not chemically interact with the biopolymers. The optimal bead consisted of 0.3–0.6% w/v chitosan, 3.9–5.1% w/v pectin, and 8.0–17.0% w/v $CaCl_2$, which yielded a high encapsulation efficiency (62.16–79.06%) and cumulative release efficiency (31.55–37.81%) after storage at 5 °C for 15 days. The antimicrobial inhibition of chitosan–pectin hydrogel beads increased with increased weight of beads. An inhibition effect against *B. cereus*, *C. perfringens*, *E. coli*, *P. fluorescens*, *L. monocytogenes* and *S. aureus* but not *Lb. plantarum* and *S.* Typhimurium was provided when the GEO+HBEO beads (4.4 g) were packed in a sachet bag. These findings suggest that chitosan–pectin hydrogel beads containing combined GEO+HBEO may be useful as a natural food preservative in food packaging systems to provide microbiological safety. Further studies will be needed to evaluate the influence of chitosan–pectin hydrogel beads containing combined EOs on the food product shelf life extension and consumer perception of ready-to-eat refrigerated foods packed with the developed beads.

Acknowledgments

This study was financially supported by Research and Researchers for Industries (RRI) (PDH58I0038), the Thailand Research Fund. Laboratory facilities were provided by the Product Development Technology Division (Faculty of Agro-Industry) and Clinical Microbiology Division (Faculty of Associated Medical Science), Chiang Mai University, Thailand.

Conflict of interest

None.

References

Ahmed, E.M. (2015). Hydrogel: preparation, characterization, and applications: a review. *Journal of Advanced Research*, **6**, 105–121.

Bagheri, H., Manap, M.Y.B.A. & Solati, Z. (2014). Antioxidant activity of *Piper nigrum* L. essential oil extracted by supercritical CO_2 extraction and hydro-distillation. *Talanta*, **121**, 220–228.

Bahmani, K., Bhatt, D.C. & Saharan, P. (2015). Evaluation of alginate beads of an antiulcer drug using experimental design: formulation and in vitro evaluation. *Der Pharmacia Lettre*, **7**, 338–343.

Bakry, A.M., Abbas, S., Ali, B. *et al*. (2016). Microencapsulation of oils: a comprehensive review of benefits, techniques, and applications. *Comprehensive Reviews in Food Science and Food Safety*, **15**, 143–182.

Balamurughan, M.G., Mohanraj, S., Kodhaiyolii, S. & Pugalenthi, V. (2014). *Ocimum sanctum* leaf extract mediated green synthesis of iron oxide nanoparticles: spectroscopic and microscopic studies. *Journal of Chemical and Pharmaceutical Sciences*, **4**, 201–204.

Bannikova, A., Rasumova, L., Evteev, A., Evdokimov, I. & Kasapis, S. (2017). Protein-loaded sodium alginate and carboxymethyl cellulose beads for controlled release under simulated gastrointestinal conditions. *International Journal of Food Science and Technology*, **52**, 2171–2179.

Benavides, S., Cortés, P., Parada, J. & Franco, W. (2016). Development of alginate microspheres containing thyme essential oil using ionic gelation. *Food Chemistry*, **204**, 77–83.

Bera, R., Mandal, B., Bhowmik, M. *et al*. (2009). Formulation and *in vitro* evaluation of sunflower oil entrapped within buoyant beads of furosemide. *Scientia Pharmaceutica*, **77**, 669–678.

Boukhatem, M.N., Kameli, A. & Saidi, F. (2013). Essential oil of Algerian rose-scented geranium (*Pelargonium graveolens*): chemical composition and antimicrobial activity against food spoilage pathogens. *Food Control*, **34**, 208–213.

Bustamante, A., Hinojosa, A., Robert, P. & Escalona, V. (2017). Extraction and microencapsulation of bioactive compounds from pomegranate (*Punica granatum* var. Wonderful) residues. *International Journal of Food Science and Technology*, **52**, 1452–1462.

Calo, J.R., Crandall, P.G., O'Bryan, C.A. & Ricke, S.C. (2015). Essential oils as antimicrobials in food systems – A review. *Food Control*, **54**, 111–119.

Calvo-Gómez, O., Morales-López, J. & López, M.G. (2004). Solid-phase microextraction–gas chromatographic–mass spectrometric

analysis of garlic oil obtained by hydrodistillation. *Journal of Chromatography A*, **1036**, 91–93.
Chang, Y., Choi, I., Cho, A.R. & Han, J. (2017). Reduction of *Dickeya chrysanthemi* on fresh-cut iceberg lettuce using antimicrobial sachet containing microencapsulated oregano essential oil. *LWT - Food Science and Technology*, **82**, 361–368.
Chouhan, S., Sharma, K. & Guleria, S. (2017). Antimicrobial activity of some essential oils—Present status and future perspectives. *Medicines*, **4**, 58.
Deladino, L., Anbinder, P.S., Navarro, A.S. & Martino, M.N. (2008). Encapsulation of natural antioxidants extracted from *llex paraguariensis*. *Carbohydrate Polymers*, **71**, 126–134.
Divya, B.J., Suman, B., Venkataswamy, M. & Thyagaraju, K. (2017). A study on phytochemicals, functional groups and mineral composition of *Allium sativum* (garlic) cloves. *International Journal of Current Pharmaceutical Research*, **9**, 42–45.
El-Kamel, A.H., Al-Gohary, O.M.N. & Hosny, E.A. (2003). Alginate-diltiazem hydrochloride beads: optimization of formulation factors, *in vitro* and *in vivo* availability. *Journal of Microencapsulation*, **20**, 211–225.
Getachew, A.T. & Chun, B.S. (2016). Optimization of coffee oil flavor encapsulation using response surface methodology. *LWT - Food Science and Technology*, **70**, 126–134.
Haghighi-Manesh, S. & Azizi, M.H. (2017). Active packaging systems with emphasis on its applications in dairy products. *Journal of Food Process Engineering*, **40**, e12542.
Han, J.H., Patel, D., Kim, J.E. & Min, S.C. (2014). Retardation of *Listeria monocytogenes* growth in mozzarella cheese using antimicrobial sachets containing rosemary oil and thyme oil. *Journal of Food Science*, **79**, E2272–E2278.
He, M., Wang, H., Dou, W., Chou, G., Wei, X. & Wang, Z. (2016). Preparation and drug release properties of norisoboldine-loaded chitosan microspheres. *International Journal of Biological Macromolecules*, **91**, 1101–1109.
Hu, R. (1999). *Food Product Design: A Computer-Aided Statistical Approach*. Pp. 23–34. Lancaster: Technomic Publishing.
Hyldgaard, M., Mygind, T. & Meyer, R.L. (2012). Essential oils in food preservation: mode of action, synergies, and interactions with food matrix components. *Frontiers in Microbiology*, **3**, 12.
Jaya, S., Durance, T.D. & Wang, R. (2009). Effect of alginate-pectin composition on drug release characteristics of microcapsules. *Journal of Microencapsulation*, **26**, 143–153.
Katata-Seru, L., Lebepe, T.C., Aremu, O.S. & Bahadur, I. (2017). Application of Taguchi method to optimize garlic essential oil nanoemulsions. *Journal of Molecular Liquids*, **244**, 279–284.
Khan, A.D. & Bajpai, M. (2011). Formulation and evaluation of floating beads of verapamil hydrochloride. *International Journal of PharmTech Research*, **3**, 1537–1546.
Khan, A., Ahmad, A., Akhtar, F. *et al*. (2010). *Ocimum sanctum* essential oil and its active principles exert their antifungal activity by disrupting ergosterol biosynthesis and membrane integrity. *Research in Microbiology*, **161**, 816–823.
Kim, T.H., Park, Y.H., Kim, K.J. & Cho, C.S. (2003). Release of albumin from chitosan-coated pectin beads in vitro. *International Journal of Pharmaceutics*, **250**, 371–383.
Kim, J.U., Kim, B., Shahbaz, H.M., Lee, S.H., Park, D. & Park, J. (2017). Encapsulation of probiotic *Lactobacillus acidophilus* by ionic gelation with electrostatic extrusion for enhancement of survival under simulated gastric conditions and during refrigerated storage. *International Journal of Food Science and Technology*, **52**, 519–530.
Konovalova, M.V., Markov, P.A., Durnev, E.A., Kurek, D.V., Popov, S.V. & Varlamov, V.P. (2017). Preparation and biocompatibility evaluation of pectin and chitosan cryogels for biomedical application. *Journal of Biomedical Materials Research A*, **105**, 547–556.
Kwiecień, I. & Kwiecień, M. (2018). Application of polysaccharide-based hydrogels as probiotic delivery systems. *Gels*, **4**, 47.
Lu, H., Shao, X., Cao, J., Ou, C. & Pan, D. (2016). Antimicrobial activity of eucalyptus essential oil against *Pseudomonas in vitro* and potential application in refrigerated storage of pork meat. *International Journal of Food Science and Technology*, **51**, 994–1001.
Molina-Calle, M., Priego-Capote, F. & Luque de Castro, M.D. (2017). Headspace-GC–MS volatile profile of black garlic vs fresh garlic: evolution along fermentation and behavior under heating. *LWT - Food Science and Technology*, **80**, 98–105.
Moreira, R.B., Teixeira, J.A., Furuyama-Lima, A.M., de Souza, N.C. & Siqueira, A.B. (2014). Preparation, characterization and evaluation of drug-delivery systems: pectin and mefenamic acid films. *Thermochimica Acta*, **590**, 100–106.
de Moura, S.C.S.R., Berling, C.L., Germer, S.P.M., Alvim, I.D. & Hubinger, M.D. (2018). Encapsulating anthocyanins from *Hibiscus sabdariffa* L. calyces by ionic gelation: pigment stability during storage of microparticles. *Food Chemistry*, **241**, 317–327.
Naganawa, R., Iwata, N., Ishikawa, K., Fukuda, H., Fujino, T. & Suzuki, A. (1996). Inhibition of microbial growth by ajoene, a sulfur-containing compound derived from garlic. *Applied and Environmental Microbiology*, **62**, 4238–4242.
Nazarudin, M.F., Shamsuri, A.A. & Shamsudin, M.N. (2011). Physicochemical Characterization of chitosan/agar blend gel beads prepared via the interphase method with different drying techniques. *International Journal of Pure and Applied Sciences and Technology*, **3**, 35–43.
Nedorostova, L., Kloucek, P., Kokoska, L., Stolcova, M. & Pulkrabek, J. (2009). Antimicrobial properties of selected essential oils in vapour phase against foodborne bacteria. *Food Control*, **20**, 157–160.
Nielsen, C.K., Kjems, J., Mygind, T. *et al*. (2017). Antimicrobial effect of emulsion-encapsulated isoeugenol against biofilms of food pathogens and spoilage bacteria. *International Journal of Food Microbiology*, **242**, 7–12.
Pandey, A.K., Sing, P. & Tripathi, N.N. (2014). Chemistry and bioactivities of essential oils of some *Ocimum* species: an overview. *Asian Pacific Journal of Tropical Biomedicine*, **4**, 682–694.
Passarinho, A.T.P., Dias, N.F., Camilloto, G.P. *et al*. (2014). Sliced bread preservation through oregano essential oil-containing sachet. *Journal of Food Process Engineering*, **37**, 53–62.
Pawar, A.P., Gadhe, A., Venkatachalam, P., Sher, P. & Mahadik, K. (2008). Effect of core and surface cross-linking on the entrapment of metronidazole in pectin beads. *Acta Pharmaceutica*, **58**, 78–85.
Peng, C., Zhao, S., Zhang, J., Huang, G., Chen, L. & Zhao, F. (2014). Chemical composition, antimicrobial property and microencapsulation of mustard (*Sinapis alba*) seed essential oil by complex coacervation. *Food Chemistry*, **165**, 560–568.
Phanthong, P., Lomarat, P., Chomnawang, M.T. & Bunyapraphatsara, N. (2013). Antibacterial activity of essential oils and their active components from Thai spices against foodborne pathogens. *ScienceAsia*, **39**, 472–476.
Rattanachaikunsopon, P. & Phumkhachorn, P. (2008). Diallyl sulfide content and antimicrobial activity against food-borne pathogenic bacteria of chives (*Allium schoenoprasum*). *Bioscience, Biotechnology, and Biochemistry*, **72**, 2987–2991.
Raut, J.S. & Karuppayil, S.M. (2014). A status review on the medicinal properties of essential oils. *Industrial Crops and Products*, **62**, 250–264.
Sajomsang, W., Nuchuchua, O., Gonil, P. *et al*. (2012). Water-soluble β-cyclodextrin grafted with chitosan and its inclusion complex as a mucoadhesive eugenol carrier. *Carbohydrate Polymers*, **89**, 623–631.
Sangsuwan, J., Pongsapakworawat, T., Bangmo, P. & Sutthasupa, S. (2016). Effect of chitosan beads incorporated with lavender or red thyme essential oils in inhibiting *Botrytis cinerea* and their

application in strawberry packaging system. *LWT - Food Science and Technology*, **74**, 14–20.
Shah, B., Davidson, P.M. & Zhong, Q. (2013). Nanodispersed eugenol has improved antimicrobial activity against *Escherichia coli* O157:H7 and *Listeria monocytogenes* in bovine milk. *International Journal of Food Microbiology*, **161**, 53–59.
Shi, J., Alves, N.M. & Mano, J.F. (2008). Chitosan coated alginate beads containing poly(*N*-isopropylacrylamide) for dual-stimuli-responsive drug release. *Journal of Biomedical Materials Research B: Applied Biomaterials*, **848**, 595–603.
Singh, P., Medronho, B., Alves, L., da Silva, G.J., Miguel, M.G. & Lindman, B. (2017). Development of carboxymethyl cellulose-chitosan hybrid micro- and macroparticles for encapsulation of probiotic bacteria. *Carbohydrate Polymers*, **175**, 87–95.
de Souza, J.R.R., de Carvalho, J.I.X., Trevisan, M.T.S., de Paula, R.C.M., Ricardo, N.M.P.S. & Feitosa, J.P.A. (2009). Chitosan-coated pectin beads: characterization and *in vitro* release of mangiferin. *Food Hydrocolloids*, **23**, 2278–2286.
Sriwattana, S., Phimolsiripol, Y., Pongsirikul, I. *et al.* (2015). Development of a concentrated strawberry beverage fortified with longan seed extract. *Chiang Mai University Journal of Natural Science*, **14**, 175–188.
Sutaphanit, P. & Chitprasert, P. (2014). Optimisation of microencapsulation of holy basil essential oil in gelatin by response surface methodology. *Food Chemistry*, **150**, 313–320.
Torpol, K., Wiriyacharee, P., Sriwattana, S., Sangsuwan, J. & Prinyawiwatkul, W. (2018). Antimicrobial activity of garlic (*Allium sativum* L.) and holy basil (*Ocimum sanctum* L.) essential oils applied by liquid vs. vapour phases. *International Journal of Food Science and Technology*, **53**, 2119–2128.
Trifunschi, S., Munteanu, M.F., Agotici, V., Pintea (Ardelean), S. & Gligor, R. (2015). Determination of flavonoid and polyphenol compounds *in Viscum album* and *Allium sativum* extracts. *International Current Pharmaceutical Journal*, **4**, 382–385.
Vasile, F.E., Romero, A.M., Judis, M.A. & Mazzobre, M.F. (2016). *Prosopis alba* exudate gum as excipient for improving fish oil stability in alginate–chitosan beads. *Food Chemistry*, **190**, 1093–1101.
Yamani, H.A., Pang, E.C., Mantri, N. & Deighton, M.A. (2016). Antimicrobial activity of Tulsi (*Ocimum tenuiflorum*) essential oil and their major constituents against three species of bacteria. *Frontiers in Microbiology*, **7**, 681.
Yang, Z., Peng, Z., Li, J. *et al.* (2014). Development and evaluation of novel flavour microcapsules containing vanilla oil using complex coacervation approach. *Food Chemistry*, **145**, 272–277.
Zhang, L., Liu, A., Wang, W. *et al.* (2017). Characterisation of microemulsion nanofilms based on Tilapia fish skin gelatine and ZnO nanoparticles incorporated with ginger essential oil: meat packaging application. *International Journal of Food Science and Technology*, **52**, 1670–1679.
Zhu, J., Tang, C., Yin, S. & Yang, X. (2018). Development and characterisation of polylactic acid–gliadin bilayer/trilayer films as carriers of thymol. *International Journal of Food Science and Technology*, **53**, 608–618.

Supporting Information

Additional Supporting Information may be found in the online version of this article:

Figure S1. The RSM plots for % encapsulation efficiency (EE) and % cumulative release efficiency (CRE), and the overlay RSM plot to obtain the optimised beads formulation to maximise % EE and % CRE.